7630 *Inorg. Chem.* **2009**, *48*, 7630–7638
DOI: 10.1021/ic900247r

Inorganic Chemistry
Article

Design and Synthesis of Coumarin-Based Zn^{2+} Probes for Ratiometric Fluorescence Imaging

Shin Mizukami, Satoshi Okada, Satoshi Kimura, and Kazuya Kikuchi*

Division of Advanced Science and Biotechnology, Graduate School of Engineering, Osaka University, 2-1 Yamadaoka, Suita, Osaka 565-0871, Japan

Received February 5, 2009

The physiological roles of free Zn^{2+} have attracted great attention. To clarify those roles, there has been a need for ratiometric fluorescent Zn^{2+} probes for practical use. We report the rational design and synthesis of a series of ratiometric fluorescent Zn^{2+} probes. The structures of the probes are based on the 7-hydroxycoumarin structure. We focused on the relationship between the electron-donating ability of the 7-hydroxy group and the excitation spectra of 7-hydroxycoumarins, and exploited that relationship in the design of the ratiometric probes; as a result, most of the synthesized probes showed ratiometric Zn^{2+}-sensing properties. Then, we designed and synthesized ratiometric Zn^{2+} probes that can be excited with visible light, by choosing adequate substituents on coumarin dyes. Since one of the probes could permeate living cell membranes, we introduced the probe to living RAW264 cells and observed the intracellular Zn^{2+} concentration via ratiometric fluorescence microscopy. As a result, the ratio value of the probe changed quickly in response to intracellular Zn^{2+} concentration.

Introduction

Zinc is one of the most heavily studied metals in biology. The biological roles of Zn^{2+} have been studied since the 1940s; the main studies focused on its biochemical roles, either as structural elements in enzymes and transcription factors or as the catalytic elements in enzymatic activity centers.[1] These Zn^{2+}s are thought to be bound strongly to peptides or proteins. Meanwhile, the physiological roles of free Zn^{2+} have recently attracted great attention, mainly in neurology.[2] Generally, to study the physiological roles of biomolecules in living cells or tissues, it is quite useful to visualize them under microscopes; fluorescent probes are useful in this endeavor. For example, rapid progress in physiological Ca^{2+} studies has been accomplished through the use of fluorescent Ca^{2+} probes such as fura-2, fluo-3, and succeeding compounds.[3] The success of Ca^{2+} probes has, in turn, encouraged the development of fluorescent probes for other various biomolecules.

With regards to fluorescent probes for Zn^{2+},[4] the pioneering compound was TSQ (*N*-(6-methoxy-8-quinolyl)-*p*-toluenesulfonamide), as reported by Frederickson et al.[5] Although it was difficult for TSQ to be applied to live cell imaging for hydrophobicity, its hydrophilic derivative, Zinquin, enabled the fluorescence microscopic imaging of free Zn^{2+}.[6] Such quinoline-based probes are, however, excited by ultraviolet light, thus inducing cell damage and autofluorescence from fluorescent biomolecules such as flavin derivatives. Thus, the fluorescent probes for longer-wavelength excitation have been actively developed by several groups.[7−10] Since most of these probes are fluorescein-based, they are much brighter than

*To whom correspondence should be addressed. E-mail: kkikuchi@mls.eng.osaka-u.ac.jp.

(1) (a) Prasad, A. S. *Biochemistry of Zinc*; Plenum Press: New York, 1993. (b) Vallee, B. L.; Falchuk, K. H. *Physiol. Rev.* **1993**, *73*, 79–118.
(2) Frederickson, C. J.; Koh, J. -Y.; Bush, A. I. *Nat. Rev. Neurosci.* **2005**, *6*, 449–462.
(3) Kao, J. P. Y. *Methods Cell Biol.* **1994**, *40*, 155–181.
(4) See following reviews: (a) Burdette, S. C.; Lippard, S. J. *Coord. Chem. Rev.* **2001**, *216−217*, 333–361. (b) Kimura, E.; Aoki, S. *Biometals* **2001**, *14*, 191–204. (c) Kikuchi, K.; Komatsu, K.; Nagano, T. *Curr. Opin. Chem. Biol.* **2004**, *8*, 182–191. (d) Dai, Z.; Canary, J. W. *New J. Chem.* **2007**, *31*, 1708–1718.
(5) Frederickson, C. J.; Kasarskis, E. J.; Ringo, D.; Frederickson, R. E. *J. Neurosci. Methods* **1987**, *20*, 91–103.
(6) Zalewski, P. D.; Forbes, I. J.; Betts, W. H. *Biochem. J.* **1993**, *296*, 403–408.
(7) (a) Hirano, T.; Kikuchi, K.; Urano, Y.; Higuchi, T.; Nagano, T. *Angew. Chem., Int. Ed.* **2000**, *39*, 1052–1054. (b) Hirano, T.; Kikuchi, K.; Urano, Y.; Higuchi, T.; Nagano, T. *J. Am. Chem. Soc.* **2000**, *122*, 12399–12400. (c) Hirano, T.; Kikuchi, K.; Urano, Y.; Nagano, T. *J. Am. Chem. Soc.* **2002**, *124*, 6555–6562. (d) Komatsu, K.; Kikuchi, K.; Kojima, H.; Urano, Y.; Nagano, T. *J. Am. Chem. Soc.* **2005**, *127*, 10197–10204.
(8) (a) Walkup, G. K.; Burdette, S. C.; Lippard, S. J.; Tsien, R. Y. *J. Am. Chem. Soc.* **2000**, *122*, 5644–5645. (b) Burdette, S. C.; Walkup, G. K.; Spingler, B.; Tsien, R. Y.; Lippard, S. J. *J. Am. Chem. Soc.* **2001**, *123*, 7831–7841. (c) Burdette, S. C.; Frederickson, C. J.; Bu, W.; Lippard, S. J. *J. Am. Chem. Soc.* **2003**, *125*, 1778–1787. (d) Chang, C. J.; Nolan, E. M.; Jaworski, J.; Burdette, S. C.; Sheng, M.; Lippard, S. J. *Chem. Biol.* **2004**, *11*, 203–210. (e) Nolan, E. M.; Lippard, S. J. *Inorg. Chem.* **2004**, *43*, 8310–8317. (f) Nolan, E. M.; Jaworski, J.; Okamoto, K. -I.; Hayashi, Y.; Sheng, M.; Lippard, S. J. *J. Am. Chem. Soc.* **2005**, *127*, 16812–16823. (g) Nolan, E. M.; Jaworski, J.; Racine, M. E.; Sheng, M.; Lippard, S. J. *Inorg. Chem.* **2006**, *45*, 9748–9757. (h) Nolan, E. M.; Ryu, J. W.; Jaworski, J.; Feazell, R. P.; Sheng, M.; Lippard, S. J. *J. Am. Chem. Soc.* **2006**, *128*, 15517–15528.
(9) Gee, K. R.; Zhou, Z. -L.; Qian, W. -J.; Kennedy, R. *J. Am. Chem. Soc.* **2002**, *124*, 776–778.
(10) Tang, B.; Huang, H.; Xu, K. H.; Tong, L. L.; Yang, G. W.; Liu, X.; An, L. G. *Chem. Commun.* **2006**, 3609–3611.

Published on Web 07/10/2009

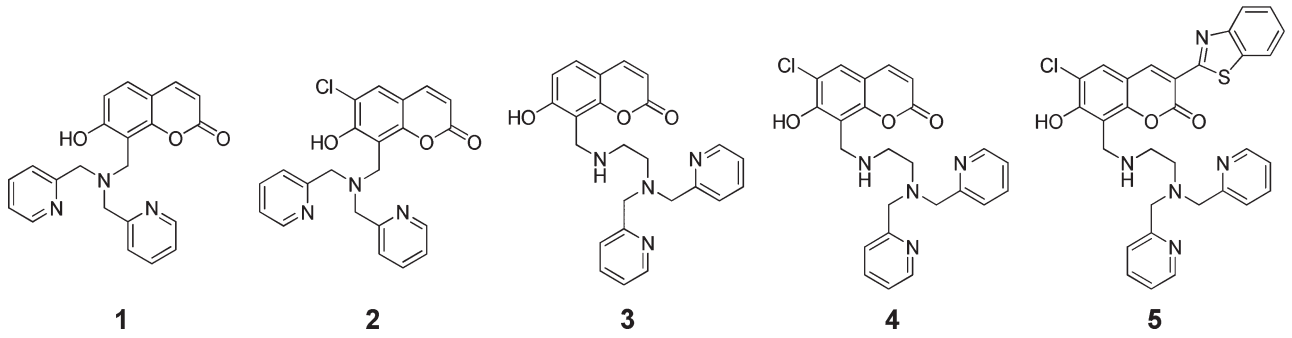

Figure 1. Structures of synthesized probes.

quinoline-based probes. Although such higher-intensity probes have several biological applications,[11] they suffer from a dependence on fluorescence intensity, in terms of dye localization or the intensity of the excitation light.

In the course of overcoming these drawbacks, ratiometric fluorescent probes for Zn^{2+} ions have been a recent focus.[12] Although there have been several ratiometric Zn^{2+} probes reported,[13] few can be practically used; in many cases, there are problems with short-wavelength excitation, low fluorescence intensity, low hydrophilicity, or elsewhere. Thus, we started developing ratiometric fluorescent Zn^{2+} probes for practical use in biological experiments.

We focused on coumarin as the fundamental platform of the fluorescent probes. Coumarins are known to be strongly fluorescent compounds, and it is easy to synthesize coumarin derivatives in general. For these reasons, coumarin-based probes are widely used in various biological assays.[14] In the case of fluorescence imaging, a coumarin-based fluorescent probe BTC is utilized for detecting Ca^{2+} in living cells.[15] Concerning Zn^{2+}-sensing probes, there have been several reports about coumarin-based fluorescent probes.[16] Brückner et al. reported of a ratiometric coumarin-based probe; however, the ratiometric property was achieved only in organic solvent.[16a,16b] In the case of other ratiometric probes, the metal selectivity and/or the cellular application was not demonstrated. Thus, there are currently no practical ratiometric Zn^{2+} probes based on a coumarin structure. Although recently Nagano et al. reported of a ratiometric probe based on an iminocoumarin structure,[13f] an iminocoumarin structure is potentially labile against hydrolysis. Therefore, there is still a great demand for ratiometric Zn^{2+} probes that can be used in imaging. We report here the design, synthesis, and photophysical properties of a series of ratiometric fluorescent Zn^{2+} probes based on a 7-hydroxycoumarin structure, after having investigated the cell membrane permeability and the ability to use Zn^{2+} in the ratiometric fluorescence imaging of living cells.

Results

Synthesis of Probes. First, we designed and synthesized a prototypical probe **1**, in only one step, from commercial compounds by using a Mannich-type reaction (Figure 1). We also designed and synthesized probes **2**−**5** by changing the ligand structure or substituting a coumarin structure (Figure 1). In the case of probe **2**, we introduced a chlorine atom at the 6-position for decreasing the pK_a of the 7-hydroxy group. In probe **3**, the ligand structure was modified; this substitution was expected to affect both the Zn^{2+}-binding affinity and the pK_a of the 7-hydroxy group. In probe **4**, we expected a cooperative effect from the introduced chlorine atom and the change in ligand structure. In probe **5**, a further substitution of a benzothiazolyl group was given at the 3-position of **4**. 3-Benzothiazolylcoumarin is the basic structure of a ratiometric Ca^{2+} probe BTC,[15] which can be excited with visible light; it is already in practical use. Thus, **5** was expected to be excited at the visible wavelength. Detailed synthesis schemes and procedures are described in the Supporting Information section.

Photophysical Properties of Probes. The excitation, emission, and absorption spectra of the prototypical probe **1** were measured (Figures 2(a), 3(a), and Supporting Information, Figure S1(a), respectively). The absorption spectra shifted toward longer wavelengths with the addition of Zn^{2+}, in a concentration-dependent manner. The peak top shifted from 331 to 357 nm. The maximum excitation wavelength also shifted with the addition of Zn^{2+}, and the fluorescence intensity largely increased. The emission spectra scarcely shifted ($\lambda_{max} \approx 450$ nm) because of the Zn^{2+} addition.

Meanwhile, the absorption and excitation spectra of the 6-chlorinated probe **2** showed a blue shift (λ_{ex}: 368 nm→ 362 nm, λ_{abs}: 367 nm → 360 nm) with the addition of Zn^{2+} (Figures 2(b) and Supporting Information, Figure S1(b)). The emission spectra also slightly shifted toward

(11) (a) Ueno, S.; Tsukamoto, M.; Hirano, T.; Kikuchi, K.; Yamada M. K.; Nishiyama, N.; Nagano, T.; Matsuki, N.; Ikegaya, Y. *J. Cell Biol.* **2002**, *158*, 215–220. (b) Qian, J.; Noebels, J. L. *J. Physiol.* **2005**, *566*, 747–758. (c) Yamasaki, S.; Sakata-Sogawa, K.; Hasegawa, A.; Suzuki, T.; Kabu, K.; Sato, E.; Kurosaki, T.; Yamashita, S.; Tokunaga, M.; Nishida, K.; Hirano, T. *J. Cell Biol.* **2007**, *177*, 637–645.

(12) See the following review: Carol, P.; Sreejith, S.; Ajayaghosh, A. *Chem. Asian J.* **2007**, *2*, 338–348.

(13) (a) Maruyama, S.; Kikuchi, K.; Hirano, T.; Urano, Y.; Nagano, T. *J. Am. Chem. Soc.* **2002**, *124*, 10650–10651. (b) Woodroofe, C. C.; Lippard, S. J. *J. Am. Chem. Soc.* **2003**, *125*, 11458–11459. (c) Chang, C. J.; Jaworski, J.; Nolan, E. M.; Sheng, M.; Lippard, S. J. *Proc. Natl. Acad. Sci. U.S.A.* **2004**, *101*, 1129–1134. (d) Taki, M.; Wolford, J. L.; O'Halloran, T. V. *J. Am. Chem. Soc.* **2004**, *126*, 712–713. (e) Kiyose, K.; Kojima, H.; Urano, Y.; Nagano, T. *J. Am. Chem. Soc.* **2006**, *128*, 6548–6549. (f) Komatsu, K.; Urano, Y.; Kojima, H.; Nagano, T. *J. Am. Chem. Soc.* **2007**, *129*, 13447–13454. (g) Zhang, Y.; Guo, X.; Si, W.; Jia, L.; Qian, X. *Org. Lett.* **2008**, *10*, 473–476. (h) Taki, M.; Watanabe, Y.; Yamamoto, Y. *Tetrahedron Lett.* **2009**, *50*, 1345–1347.

(14) (a) Goddard, J. P.; Raymond, J. L. *Trends Biotechnol.* **2004**, *22*, 363–370. (b) Katerinopoulos, H. E. *Curr. Pharm. Des.* **2004**, *10*, 3835–3852.

(15) Itaridou, H.; Foukaraki, E.; Kuhn, M. A.; Marcus, E. M.; Haugland, R. P.; Katerinopoulos, H. E. *Cell Calcium* **1994**, *15*, 190–198.

(16) (a) Lim, N. C.; Brückner, C. *Chem. Commun.* **2004**, 1094–1095. (b) Lim, N. C.; Schuster, J. V.; Porto, M. C.; Tanudra, M. A.; Yao, L.; Freake, H. C.; Brückner, C. *Inorg. Chem.* **2005**, *44*, 2018–2030. (c) Dakanali, M.; Roussakis, E.; Kay, A. R.; Katerinopoulos, H. E. *Tetrahedron Lett.* **2005**, *45*, 4193–4196. (d) Kulatilleke, C. P.; de Silva, S. A.; Eliav, Y. *Polyhedron* **2006**, *25*, 2593–2596. (e) Zhang, L.; Dong, S.; Zhu, L. *Chem. Commun.* **2007**, 1891–1893.

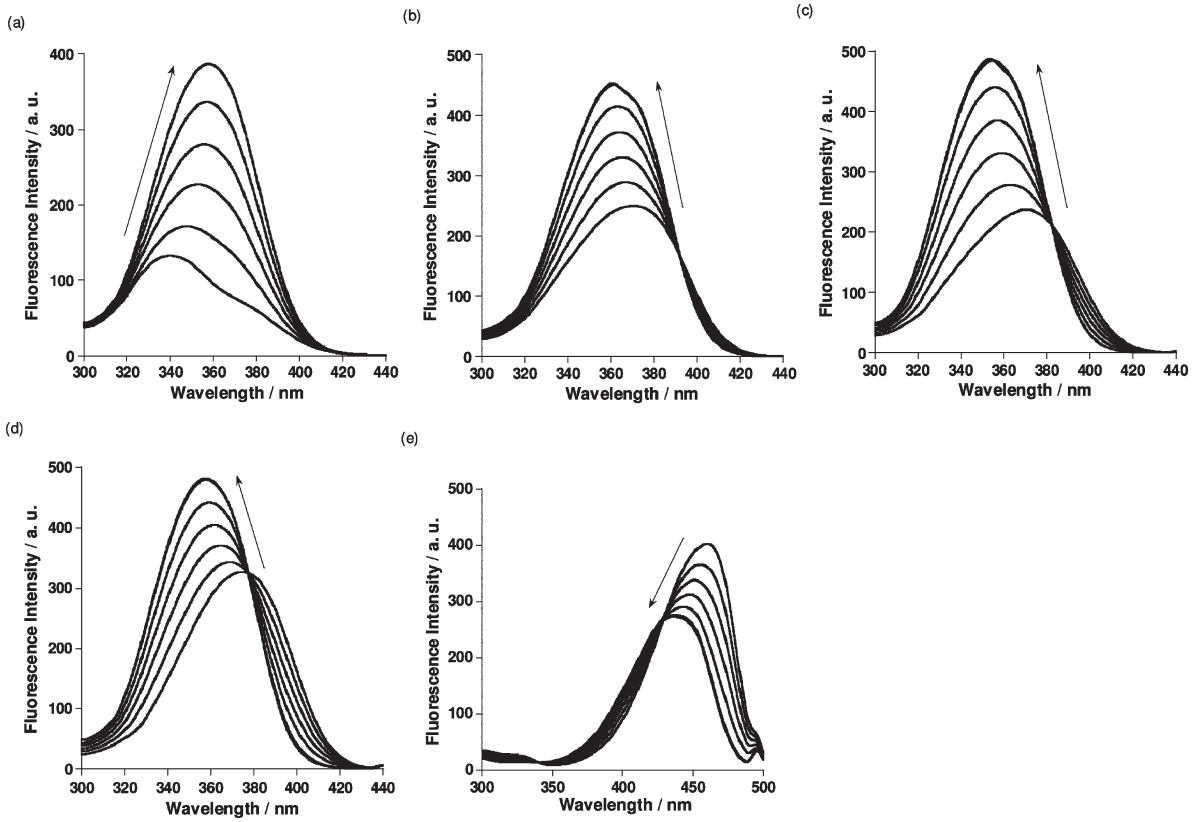

Figure 2. Excitation spectra of (a) 5 μM **1** (λ_{em} = 450 nm), (b) 5 μM **2** (λ_{em} = 445 nm), (c) 5 μM **3** (λ_{em} = 440 nm), (d) 5 μM **4** (λ_{em} = 443 nm), and (e) 1 μM **5** (λ_{em} = 494 nm), in the presence of various concentrations of Zn^{2+} (0, 0.2, 0.4, 0.6, 0.8, and 1.0 equiv to the probe concentration) in 100 mM HEPES buffer solution (pH 7.4). Arrows indicate the directions of the spectral changes as Zn^{2+} concentration increased.

shorter wavelengths, because of the Zn^{2+} addition (Figure 3(b)). The excitation, emission, and absorption spectra of **3**−**5** also showed blue shifts on account of adding Zn^{2+} (Figures 2(c)−(e), 3(c)−(e), and Supporting Information, Figure S1(c)−(e)).

We also investigated the fluorescence quantum yields of the synthesized compounds in the free form versus the Zn^{2+} complex form. The fluorescence quantum yields of probes **1**−**4** were increased by complexation with Zn^{2+}; all but **5** showed a remarkable change in fluorescence quantum yield. The photophysical data for the synthesized probes are summarized in Table 1.

Effect of pH on Photophysical Properties of Probes. We investigated the effect of solution pH on the photophysical properties of the synthesized probes. The absorption spectra of **1** at various solution pHs are shown in Figure 4(a). In acidic solution, the maximum absorption wavelength was at around 326 nm; in basic solution, however, the peak top shifted to 377 nm. In the case of probes **2**−**5**, their absorption spectra also showed red shifts as solution pH increased (Supporting Information, Figure S2).

Next, the effect of pH on the excitation spectrum of **1** was investigated. The fluorescence spectra of **1** at various solution pHs are shown in Figure 4(b). When the solution pH was increased from an acidic value, the fluorescence intensity increased; this trend continued until the pH was neutral, and the intensity then decreased when the pH was in excess of 8.

The fluorescence intensity of probes **1**−**5** at several solution pH points are plotted in Figure 4(c). Concerning all synthesized probes, the fluorescence intensity values decreased in the acidic and basic regions, although a control compound—7-hydroxy-8-methylcoumarin (HMC), which lacks a DPA ligand—did not show a fluorescence decrease at a basic-solution pH. Most probes, with the exception of **2**, showed virtually no physiological pH-sensitivity in the pH region of 7.4. The pK_a values of probes **1**−**5** were determined by pH titrating absorption measurements (Table 1). We also carried out potentiometric titration experiments (Supporting Information, Figure S5). For each compound, the pK_a value determined by absorbance titration was roughly consistent with one of the pK_a values determined by potentiometric titration (Supporting Information, Table S1).

Metal-Binding Properties. (1). Stoichiometry of Binding to Zn^{2+}. The binding stoichiometry of the probes to Zn^{2+} was investigated by Job's plot.[17] It was confirmed that all probes form 1:1 complexes with Zn^{2+} (Supporting Information, Figure S3).

(2). Apparent Binding Constants to Zn^{2+}. The apparent dissociation constants (K_d) of probes **1**−**5** in neutral aqueous buffer were determined by plotting the fluorescence intensity to free Zn^{2+} concentration (Supporting Information, Figure S4). The K_d values of probes **1**−**5** were in the range of 3.6−28 pM, as shown in Table 1.

(3). Metal-Sensing Selectivity. We investigated the fluorescence ratio values of the probes in response to various metal ions (Figure 5). The results of probes **1**−**4**

(17) Job, P. *Ann. Chim.* **1928**, *9*, 113–203.

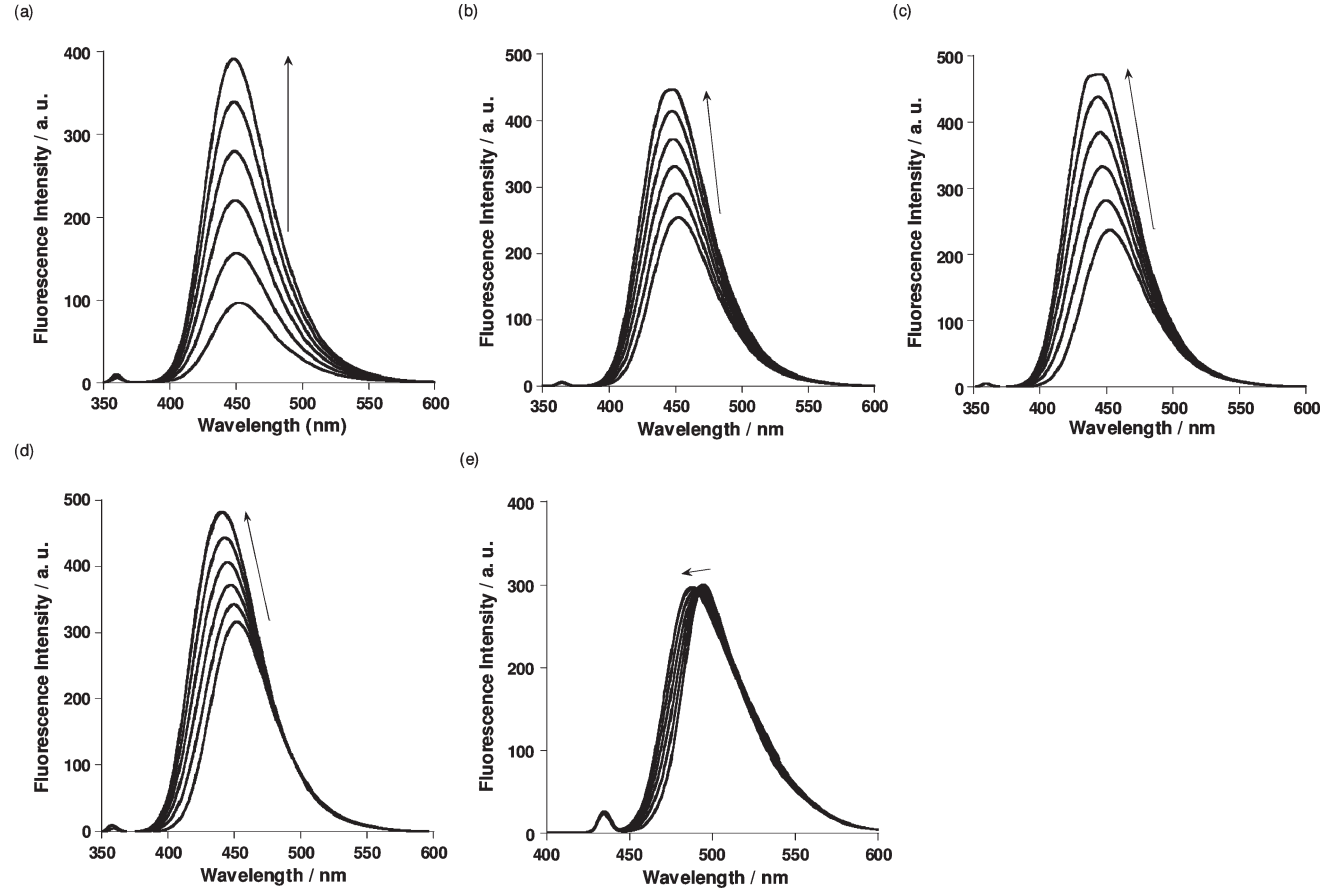

Figure 3. Emission spectra of (a) 5 μM **1** (λ_{ex} = 358 nm), (b) 5 μM **2** (λ_{ex} = 362 nm), (c) 5 μM **3** (λ_{ex} = 357 nm), (d) 5 μM **4** (λ_{ex} = 357 nm), and (e) 1 μM **5** (λ_{ex} = 432 nm), in the presence of various concentrations of Zn^{2+} (0, 0.2, 0.4, 0.6, 0.8, and 1.0 equiv to the probe concentration) in 100 mM HEPES buffer solution (pH 7.4). Arrows indicate the directions of the spectral changes as Zn^{2+} concentration increased.

Table 1. Physical Properties of Synthesized Probes

	absorption				excitation		emission		quantum yield			
	λ_{max}/nm ε/M^{-1} cm^{-1}				λ_{max}/nm		λ_{max}/nm		Φ		dissociation constant to Zn^{2+}	
compound	free		Zn^{2+}		free	Zn^{2+}	free	Zn^{2+}	free	Zn^{2+}	K_d/pM	pK_a[a]
1	331	12,300	357	16,500	344	358	451	450	0.41	0.66	28	8.9
2	367	15,100	360	17,600	368	362	450	445	0.51	0.71	14	4.0
3	369	14,100	351	18,000	374	357	452	443	0.46	0.83	5.2	6.3
4	372	19,700	354	19,100	374	357	450	440	0.52	0.80	5.0	3.7
5	442	51,500	423	48,500	454	432	494	487	> 0.96	> 0.99	3.6	2.5

[a] pK_a values determined by absorbance titration.

were quite similar to those of other probes that have a dipicolylamino group as the ligand. The fluorescence ratio values of all compounds were not affected by physiologically abundant metal ions such as Na^+, K^+, Mg^{2+}, or Ca^{2+}, even when the concentration of those metal ions were 5 mM—although Cd^{2+} also changed the fluorescence spectra. Regarding transition metals, Fe^{3+}, Co^{2+}, Ni^{2+}, and Cu^{2+} caused a quenching of the fluorescence.

Ratiometric Zn^{2+} Imaging in Living Cells. For the biological application, we first investigated cell permeability. RAW264 cells were incubated with our synthesized probes; of the five probes, only **5** successfully permeated the cells (Figure 6(a)). The ratiometric fluorescence images of the same picture as in Figure 6(a) were shown in Figure 6(b) top, where the cells were excited at two excitation wavelengths, 380 and 450 nm; the fluorescence ratio values were calculated with imaging software. Next, we investigated the Zn^{2+}-sensing ability of **5** in living cells. A total of 5 μM pyrithione as a Zn^{2+} ionophore and 50 μM Zn^{2+} were added to the cells, to increase the intracellular Zn^{2+} concentration $[Zn^{2+}]_i$. The ratio fluorescence values (F_{380}/F_{450}) were increased gradually, and became constant within several minutes; the pseudocolor changed purple or blue to yellow or green, which means the increase of the ratio fluorescence values (Figure 6(b) middle). Then, 100 μM TPEN (*N*,*N*,*N*′,*N*′-tetrakis(2-pyridylmethyl)ethylenediamine) was added, to decrease free $[Zn^{2+}]_i$ by chelating Zn^{2+}. The ratio fluorescence values were decreased to the background level with

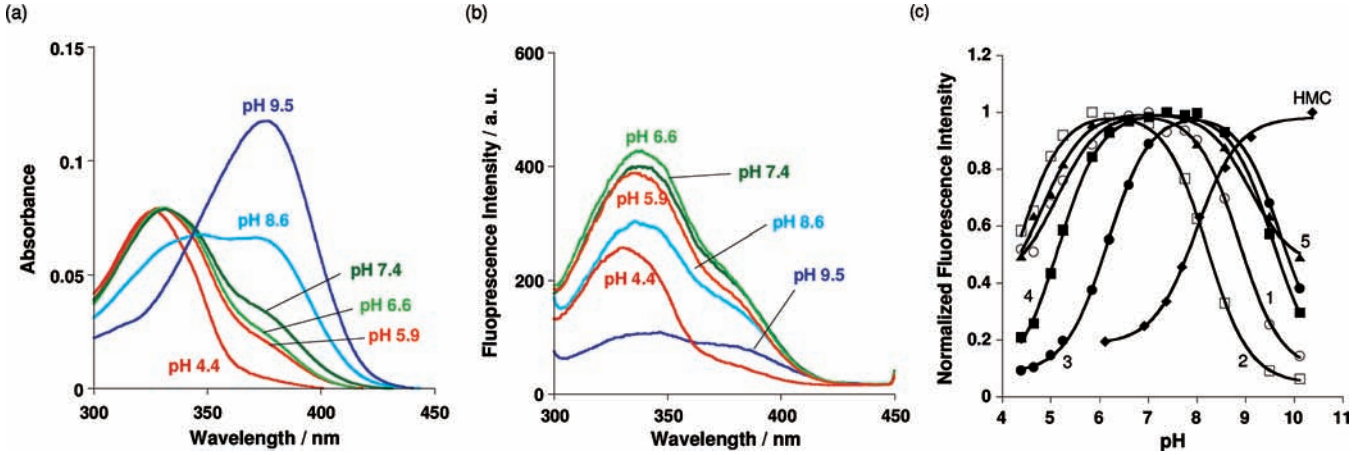

Figure 4. (a) Absorption and (b) excitation spectra (λ_{em} = 451 nm) of **1** at various solution pHs. (c) Effect of pH on fluorescence intensity of synthesized probes.

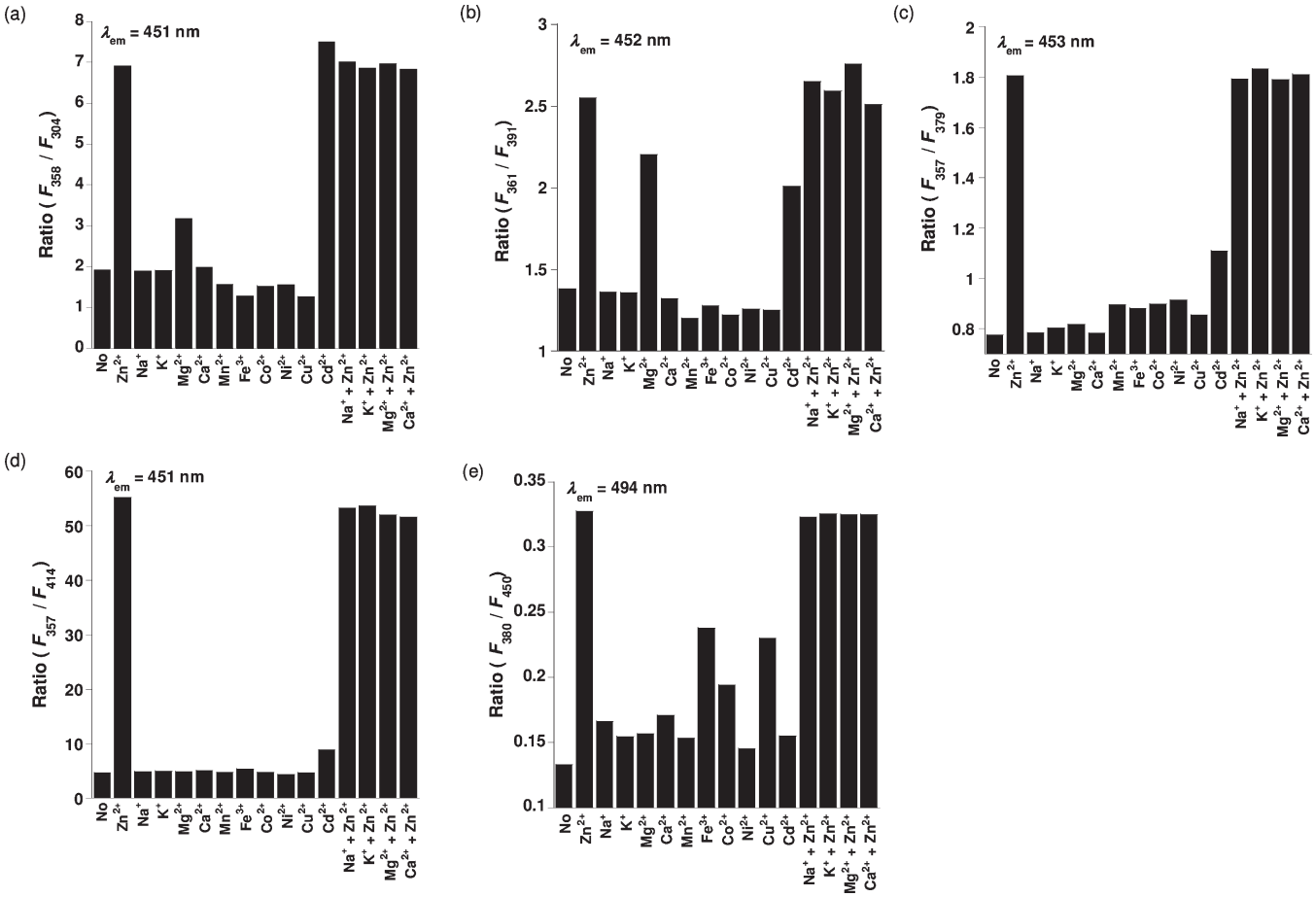

Figure 5. Metal-sensing selectivity of compounds (a) **1**, (b) **2**, (c) **3**, (d) **4**, and (e) **5**. F_x: fluorescence intensity excited at x nm. Na^+, K^+, Mg^{2+}, and Ca^{2+} were added at 1,000 times the concentration of the probes. Zn^{2+}, Mn^{2+}, Fe^{3+}, Ni^{2+}, Co^{2+}, Cu^{2+}, and Cd^{2+} were added at the equivalent concentration of the probes.

the pseudocolor getting back to the initial color (Figure 6(b) bottom). The time course of the fluorescence ratio values in three different areas indicated in Figure 6(a) were shown in Figure 6(c).

Discussion

Design of Prototypical Probe 1. First, we designed **1** as a prototypical compound of coumarin-based ratiometric Zn^{2+} probes (Figure 1). As the chromophore, we chose 7-hydroxycoumarin, also called umbelliferone, because of its strong fluorescence intensity and easy synthesis. As the metal ligand, a dipicolylamine (DPA) structure was chosen because of its high specificity, high stability, and fast complexation ability with Zn^{2+}. Although coumarin-based Zn^{2+} probes with a DPA ligand have been reported,[16b,16d] they did not exhibit ratiometric fluorescent

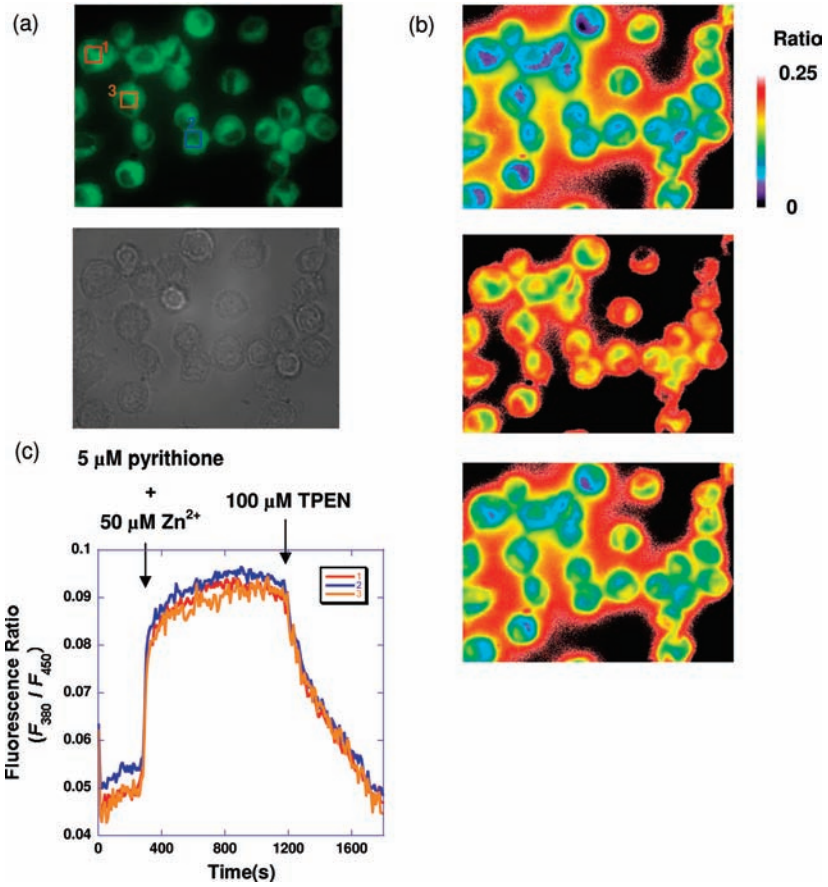

Figure 6. (a) Fluorescence microscopic image (λ_{ex}: 450 nm) (top), brightfield microscopic image (bottom), and (b) ratiometric fluorescence image (λ_{ex}: 380 and 450 nm) of RAW264 cells (top: 0 s, middle: 600 s, bottom: 1800 s) incubated with 10 μM **5** for 5 min at 37 °C. The color coding scale means the fluorescence ratio values. (c) Time course of the ratiometric fluorescence values of the areas 1 (red), 2 (blue), and 3 (orange), which are indicated in (a).

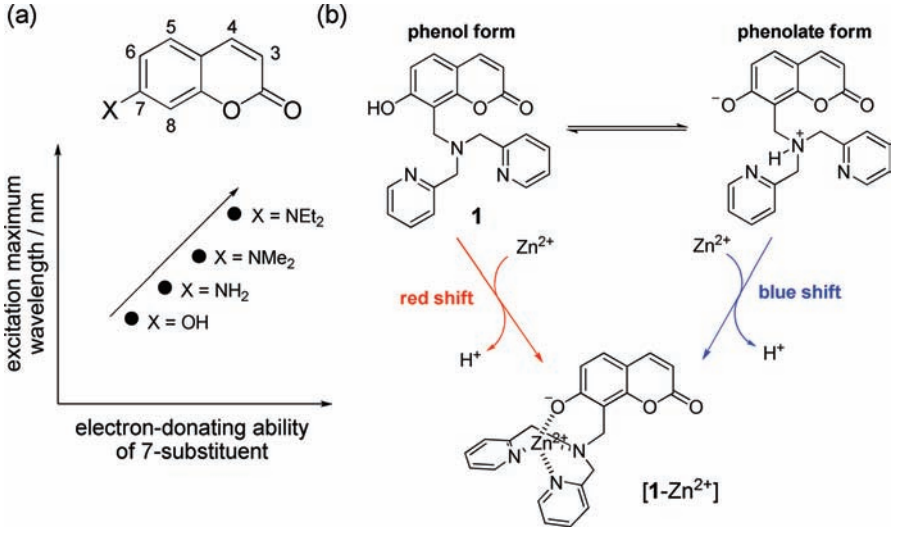

Figure 7. (a) Correlation between the electron-donating ability of 7-substituent and the excitation maximum wavelength of 7-substituted coumarins. (b) Two forms of probe **1** and the spectral change to the Zn^{2+} complex.

properties under physiological conditions. To achieve ratiometric Zn^{2+}-sensing, we focused our attention on the spectroscopic property of 7-substituted coumarins. As we had previously utilized the property for anion-sensing,[18] the absorbance and excitation spectra of the 7-substituted coumarin were affected by the functional substitution at the 7-position (Figure 7(a)).[19] When the oxygen atom of 7-hydroxy group coordinates Zn^{2+}, the absorption and the excitation spectra are expected to shift toward either

(18) Mizukami, S.; Nagano, T.; Urano, Y.; Odani, A.; Kikuchi, K. *J. Am. Chem. Soc.* **2002**, *124*, 3920–3924.

(19) Wheelock, C. E. *J. Am. Chem. Soc.* **1959**, *81*, 1348–1352.

longer or shorter wavelengths, according to changes in electron-donating ability. The direction of the excitation spectral shift would be dependent on whether the 7-hydroxy group is protonated or deprotonated under the measurement condition. Since the electron-donating ability is expected to be increased in the order of $-OH < -O^-\cdots Zn^{2+} < -O^-$, we expected spectral changes as follows: When the phenol form is dominant, the complexation with Zn^{2+} would prompt red shifts in the spectra; when the phenolate form is dominant, Zn^{2+} complexation would prompt blue shifts (Figure 7(b)).

Zn^{2+}-Sensing Properties of Probe 1. When Zn^{2+} was added to the solution of 5 μM **1**, the absorbance and the excitation spectra were shifted toward longer wavelengths (Supporting Information, Figure S1(a) and Figure 2(a), respectively). These results indicate that the 7-hydroxy group participated in the coordination with Zn^{2+}, and that the phenol form of **1** is dominant in 100 mM HEPES buffer (pH 7.4) (Figure 7(b)). This presumption was also confirmed by the pH profile measurement of the absorbance spectra (Figure 4(a)), where the peak top was around 330 nm at pH 7.4, as well as at a more acidic pH—although the peak top was around 370 nm at pH 9.5. The absorbance peak top of the 7-hydroxycoumarin was at 330 nm when the 7-hydroxy group was protonated, but shifted to 370 nm for the phenolate form.[20] According to the above mechanism, **1** made an excitation spectral shift toward a longer wavelength, with the addition of Zn^{2+} (Figure 2(a)); however, the spectral change was not ideal for ratiometric fluorescence imaging, because there was no clear isofluorescent point in the excitation spectra. On the other hand, an isosbestic point was observed in the absorbance spectra of **1** titrated with Zn^{2+} (Supporting Information, Figure S1(a)). This would be ascribed to the fluorescence quenching of **1**, because the fluorescence quantum yield (Φ) of **1** was lower than that of [**1**$-Zn^{2+}$] (Table 1). We considered the quenching to be the result of the photoinduced electron transfer (PET) from a DPA moiety, which would have been observed in known coumarin-based Zn^{2+} probes possessing a DPA ligand.[16b,16d]

Introduction of Chlorine Atom at the 6-Position of Coumarin: Design and Properties of Probe 2. In the case of **1**, the phenol form was expected to be dominant in pH 7.4, as described above. Conversely if the phenolate form is dominant, it will induce a blue shift of the excitation spectra. We considered that the difference in the way of spectral shift might enable the ratiometric measurement. Thus, we designed compound **2**, in which a chlorine atom was introduced at the 6-position. The substitution of a chloro- or fluoro-group at the 6-position can decrease the pK_a of 7-hydroxycoumarin via the inductive effect, and it was expected that the dominant form of **2** in pH 7.4 buffer was the deprotonated one.

The excitation spectral change of **2** (Figure 2(b)) showed that Zn^{2+} induced the blue shift of the excitation spectra. Also, the pH profile of the absorbance spectra of **2** indicated that the phenolate form of **2** was the dominant species at pH 7.4 because the absorbance maximum wavelength was 372 nm (Supporting Information, Figure S2(a)). Meanwhile, the difference in excitation maximum wavelength between **2** and [**2**$-Zn^{2+}$] was only 6 nm; therefore, further improvement was desired in terms of practical ratiometric fluorescence measurement, although there was an isofluorescent point in the excitation spectral change.

Modification of the Ligand Structure: Designs and Properties of Probes 3 and 4. We attempted to change the Zn^{2+} ligand structure because the modification of the ligand structure might not only change the association constant among metal ions but also change the pK_a of the hydroxy group near the ligand. We designed **3** and **4** with another ligand, *N*,*N*-dipicolylaminoethylamine. With regards to both **3** and **4**, the phenolate forms were dominant at pH 7.4 (Supporting Information, Figures S2(b) and S2(c)), and thus the addition of Zn^{2+} induced the blue shifts in the excitation spectra, as the case of **2** (Figures 2(c) and 2(d)).

The excitation maximum wavelengths of **3** and **4** were each 374 nm. When the probes bound Zn^{2+} ions, the spectral peak tops were shifted to 357 nm, and thus the spectral shifts were 17 nm each—much larger than had been the case with **1** or **2**. In the excitation spectra of **3** and **4**, in the presence of several concentrations of Zn^{2+} ion, there were isofluorescent points at 382 and 377 nm, respectively; therefore, they could serve as more practical ratiometric probes for Zn^{2+} ions. However, they are excitable only by UV light, which can cause damage to living cells and tissues. We therefore sought to improve further the probe structure for visible light excitation.

Design and Properties of Visible Light Excitation Probe 5. To achieve longer-wavelength excitation, further modification was required. Since deprotonated 3-benzothiazolyl-7-hydroxycoumarin is known to have strong absorption in the visible light region in polar solvent,[21] we designed and synthesized **5** based on this structure. As expected, the excitation maximum of **5** was at 454 nm for the deprotonated form as well as for **3** and **4**, and at 432 nm for the Zn^{2+} complex (Figure 2(e)). The isofluorescent point of the excitation spectra was observed at 428 nm. Thus, this probe can be used for ratiometric fluorescence measurement of Zn^{2+} with visible light excitation, for example, at 400 and 450 nm. In addition to the ratiometric fluorescence property derived by exciting at two different wavelengths, probe **5** could also be applied to ratiometric measurement by monitoring at two emission wavelengths. Figure 3(e) shows the emission spectral change in the presence of Zn^{2+}; the peak top shifted from 494 to 487 nm, with an isofluorescent point at 491 nm with Zn^{2+} addition. In passing, it should be noted that probe **4** also showed the same ratiometric emission properties.

Zn^{2+}-binding Properties of Probes 1−5. To study the Zn^{2+}-binding properties of the probes, the binding stoichiometry to Zn^{2+} was investigated. Job's plots showed that all probes formed 1:1 complexes with Zn^{2+} (Supporting Information, Figure S3). The apparent dissociation constants with Zn^{2+} were as high as with the known Zn^{2+} probes. Concerning the correlation between ligand structure and the apparent binding constant to Zn^{2+}, the dipicolylaminoethylamino group showed a

(20) Fink, D. W.; Koehler, W. R. *Anal. Chem.* **1970**, *42*, 990–993.

(21) Azim, S. A.; Al-Hazmy, S. M.; Ebeid, E. M.; El-Daly, S. A. *Opt. Laser Technol.* **2005**, *37*, 245–249.

slightly higher binding constant than did the dipicolylamino group. The sensing selectivity to Zn^{2+} was sufficient for cellular application, although the ratiometric values of probes are largely changed by Cd^{2+} ions, because Cd^{2+} does not constitute an important metal ion in physiological studies. In the case of **5**, the ratio values change by a small amount in response to Fe^{3+}, Cu^{2+}, and Co^{2+}; however, it is thought that these transition metal ions are generally bound to proteins and scarcely exist as free ions.

Cellular Application. To confirm whether **5** can detect intracellular Zn^{2+} under ratiometric fluorescence microscopy, we introduced the probe to RAW264 cells. Probe **5** could pass through the cell membrane without any modifications, as shown in Figure 6(a), probably because of the high lipophilicity involved. We then measured the change in ratiometric signal F_{380}/F_{450} by changing the intracellular Zn^{2+} concentration with pyrithione and TPEN. The results (Figure 6(b) and 6(c)) indicate that the probe enables the ratiometric detection of intracellular Zn^{2+} as quickly as the reported probes.[7c,8b] Since there are few compounds that can achieve both visual light excitation and ratiometric imaging in cells, we expect this probe can be utilized for the ratiometric detection of Zn^{2+} concentration in living cells that are vulnerable to UV excitation.

Conclusion

We developed a series of coumarin-based fluorescent probes for detecting Zn^{2+} with high affinities. The design strategy was based on the fluorescent properties of 7-substituted coumarins. The ligands were introduced at the 8-position because of the ease of synthesis and the electrostatic effects in reducing the pK_a of 7-hydroxy groups. Additional substituents were incorporated into the 6- and/or 3-position to improve the properties. Among five developed probes, **2**−**5** showed the ratiometric fluorescent properties, and **5** could be excited at visible light wavelength. Using cell membrane permeable probe **5**, we confirmed the ratiometric fluorescence-sensing ability for free Zn^{2+} in living cells. We expect this probe will lead to the "next stage" of physiological Zn^{2+} studies, in both neurology and immunology, and so on.

Experimental Section

Materials and Instruments. The detailed synthesis procedures for **1**−**5** are described in Supporting Information. All reagents for synthesis and measurements were purchased from Tokyo Chemical Industries, Wako Pure Chemical, or Aldrich Chemical Co. All were of the highest grade available, and were used without further purification. Silica gel column chromatography was performed using BW-300, or Chromatorex NH (Fuji Silysia Chemical Ltd.). Cells were obtained from the Riken BRC Cell Bank, and reagents for culture were purchased from Gibco. NMR spectra were recorded on a JEOL JNM-EX270 instrument at 270 MHz for ^{1}H NMR and at 64.5 MHz for ^{13}C NMR, or a JEOL JNM-AL400 instrument at 400 MHz for ^{1}H and at 100.4 MHz for ^{13}C NMR, using tetramethylsilane as an internal standard. Mass spectra (CI, FAB) were measured on a JEOL JMS-700. ESI-TOF MS was taken on a Waters LCT-Premier XE. UV−visible spectra were measured using a Shimadzu UV-1650PC. Fluorescence spectra were measured using a Hitachi F4500 spectrometer. The slit width for both excitation and emission spectra was 5.0 nm. The photomultiplier voltage was 400 V. For ratiometric fluorescence images were recorded using IX71 (Olympus) for the fluorescent microscope, Cool Snap HQ (Roper Scientific) for the cooled CCD camera, Polychrome V (TILL Photonics) for the xenon lamp with a monochromator, 470DCXRU (CHROMA) for the dichroic mirror, HQ515/50m-2p (CHROMA) for the emission filters, and MetaMorph (Universal Imaging Corporation) for the imaging software and data analysis.

Measurement of Photophysical Properties. All probes were prepared at 5 mM stock DMSO solution and diluted to the final concentration for each experiment. Zn^{2+} stock solution was prepared at 50 mM concentration by dissolving $ZnSO_4 \cdot 7H_2O$ in ultrapure water. Absorbance, excitation, and emission spectra were measured in 100 mM HEPES buffer (pH 7.4) at 25 °C. Quantum yields were calculated using quinine sulfate ($\Phi = 0.55$) in 0.5 M H_2SO_4 aq. or fluorescein ($\Phi = 0.92$) in 0.1 M NaOH aq. as the standard compounds, as described previously.[22]

Preparation of Zn^{2+}- and pH-Buffered Solution. A series of 100 mM HEPES buffer (pH 7.4, $I = 0.1$ ($NaNO_3$)) were prepared containing 10 mM nitrilotriacetic acid (NTA) and 0−5.3 mM $ZnSO_4$. The apparent stability constant for NTA-Zn^{2+} complex β_1' is defined as follows: $\beta_1' = \beta_1/\alpha_M\alpha_L$, where β_1 is the stability constant for NTA-Zn^{2+} complex, $\alpha_M = 1 + 10^{(pH - pK1)}$, $\alpha_L = 1 + 10^{(pKa1 - pH)} + 10^{(pKa1 + pKa2 - 2pH)} + 10^{(pKa1 + pKa2 + pKa3 - 3pH)}$. Regarding the p$K_a$ of Zn^{2+}, p$K_1 = 9.0$,[23] and regarding the pK_as of NTA, p$K_{a1} = 9.74$, p$K_{a2} = 2.48$, and p$K_{a3} = 1.88$.[23] Protonation constants were corrected upward by 0.11 for 0.1 M of ionic strength.[24] The stability constant for NTA-Zn^{2+} complex: $\log\beta_1 = 10.4$.[23] Thus, $\alpha_M \approx 1$, $\alpha_L \approx 10^{2.34}$. $\beta_1' = \beta_1/\alpha_M\alpha_L = 10^{10.4}/10^{2.34} = 10^{8.06}$. Free Zn^{2+} concentration $[Zn^{2+}]_{free}$ was calculated as per the following equation.

$$[Zn^{2+}]_{free} = [Zn^{2+}]_{total}/(\beta_1'\alpha_M[NTA]_{free})$$
$$= [Zn^{2+}]_{total}/\{\beta_1'\alpha_M([NTA]_{total} - [Zn^{2+}]_{total})\}$$

Determination of the Apparent Dissociation Constant (K_d) with Zn^{2+}. The fluorescence intensity F of the probes were plotted against $[Zn^{2+}]_{free}$, the concentration of free Zn^{2+}. The apparent dissociation constants K_ds with Zn^{2+} were determined by fitting the data to the following equation:

$$F = F_0 + (F_{max} - F_0)[Zn^{2+}]_{free}/(K_d + [Zn^{2+}]_{free})$$

where F is the observed fluorescence intensity, F_0 is the fluorescence intensity without Zn^{2+}, F_{max} is the maximum fluorescence intensity, and $[Zn^{2+}]_{free}$ is the concentration of free Zn^{2+}.

Effect of pH on Fluorescence Properties. We measured the fluorescence intensity of the probes in 10 mM phosphate buffer aqueous solution showing several pH values (pH 4.4−12.5). The fluorescence intensities were plotted against solution pH.

Metal Ion Selectivity. The fluorescence intensity and ratio values were measured in 100 mM HEPES buffer (pH 7.4). The probe concentration was 5 μM for **1**−**4** or 1 μM for **5**. The stock solutions of Na^+, K^+, Ca^{2+}, and Mg^{2+} were prepared at 500 mM and diluted to final concentrations (5 mM or 1 mM). The stock solution of Mn^{2+}, Fe^{3+}, Co^{2+}, Ni^{2+}, Cu^{2+}, Zn^{2+}, and Cd^{2+} were prepared at 5 mM and diluted to final concentrations (5 μM or 1 μM).

Cell Cultures and Live Cell Imaging. RAW264 cells were cultured in MEM containing 10% fetal bovine serum, 1% penicillin, 1% streptomycin, and 0.1 mM MEM non-essential amino acid solution at 37 °C in a 5% CO_2 incubator. The cells

(22) Dawson, R. W.; Windsor, W. M. *J. Phys. Chem.* **1968**, *72*, 3251–3260.
(23) Perin, D. D.; Dempsey, B. *Buffers for pH and Metal Ion Control*; John Wiley & Sons, Chapman and Hall: New York and London, 1974.
(24) Martell, A. E.; Smith, R. M. *NIST Critical Stability Constants of Metal Complexes, NIST Standard Reference Database*; Plenum Press: New York and London, 1974; Vol. *1*.

were transferred to a glass-bottomed dish and incubated for 1 day before dye-loading. The cells were washed with PBS twice and incubated with PBS containing 10 μM probes for 5 min at 37 °C. The cells were then washed with PBS twice, and measurements were carried out with fluorescence microscope. A total of 5 μM pyrithione and 50 μM Zn^{2+} were treated to increase intracellular Zn^{2+} concentration, $[Zn^{2+}]_i$, and 100 μM TPEN was treated to decrease $[Zn^{2+}]_i$ by chelating.

Acknowledgment. This work was supported in part by the Ministry of Education, Culture, Sports, Science and Technology (MEXT) of Japan (Grants 18310144, 18032045, 18033034, 18011005, 19036012, 19021028, 19651093 to K.K. and 19710185 to S.M.). This work was also supported by the Special Coordination Funds for the Council of Science and Technology Policy Coordination Program of Science and Technology Projects, MEXT and JST, to K.K. K.K. was also supported by the Mitsubishi Foundation, by the Novartis Foundation for the Promotion of Science, by Shimadzu Science Foundation, by Kato Memorial Bioscience Foundation, by Astellas Foundation for Research on Metabolic Disorders, by the Uehara Memorial Foundation, by Terumo Life Science Foundation, by Nagase Science and Technology Foundation, and by the Asahi Glass Foundation. S.M. was supported by the Cosmetology Research Foundation.

Supporting Information Available: Detailed synthetic procedures of compounds, and supplementary figures. This material is available free of charge via the Internet at http://pubs.acs.org.